10-2007

Electroelastic Effect of Thickness Mode Langasite Resonators

Haifeng Zhang
University of Nebraska - Lincoln

Joseph A. Turner
University of Nebraska - Lincoln, jaturner@unl.edu

J S. Yang
jyang1@unl.edu

J. A. Kosinski
U.S. Army Research Development and Engineering Command (RDECOM) Communications-Electronics Research, Development and Engineering Center (CERDEC), Fort Monmouth, NJ

Electroelastic Effect of Thickness Mode Langasite Resonators

Haifeng Zhang, Joseph A. Turner, Jiashi Yang, *Senior Member, IEEE*, and John A. Kosinski, *Fellow, IEEE*

***Abstract*—Langasite is a very promising material for resonators due to its good temperature behavior and high piezoelectric coupling, low acoustic loss, and high Q factor. The biasing effect for langasite resonators is crucial for resonator design. In this article, the resonant frequency shift of a thickness-mode langasite resonator is analyzed with respect to a direct current (DC) electric field applied in the thickness direction. The vibration modes of a thin langasite plate fully coated with an electrode are analyzed. The analysis is based on the theory for small fields superposed on a bias in electroelastic bodies and the first-order perturbation integral theory. The electroelastic effect of the resonator is analyzed by both analytical and finite-element methods. The complete set of nonlinear elastic, piezoelectric, dielectric permeability, and electrostrictive constants of langasite is used in the theoretical and numerical analysis. The sensitivity of electroelastic effect to nonlinear material constants is analyzed.**

I. Introduction

The electroelastic effect of piezoelectric resonators is defined as the resonant frequency shift that occurs with respect to an applied direct current (DC) electric field. This phenomenon can be explained by the nonlinear theory of piezoelectricity. This interesting effect has been applied to frequency-temperature compensation [1] and electrostatic voltage sensors [2]–[4]. A recent attempt also has been made to use the electroelastic effect to reduce the acceleration sensitivity of quartz resonators [5]. Finally, the measurement of electroelastic effect can be used to determine the third-order piezoelectric constants [6]. Although most of the applications mentioned above use quartz as the resonator material, $La_3Ga_5SiO_{14}$ single crystals are of recent interest. Langasite belongs to point group 32, such that it has the same symmetry as quartz. It has good temperature behavior and piezoelectric coupling factor, low acoustic loss, and high Q factor [7], [8]. Resonators made from this material are expected to perform better than those made from quartz [9]. The frequency shift of langasite resonators caused by temperature was investigated by Fritze *et al.* [10] and Mateescu *et al.* [11]. The force-frequency effect was studied by Kim and Ballato [12] and Kosinski *et al.* [13]. Research associated with the electroelastic effect for langasite resonators has not yet been reported.

The sensitivity of the electroelastic effect to nonlinear material constants is critical for accurate determination of nonlinear material constants by resonator methods. Related work for quartz resonators was reported by Brendel [14] for one specific cut, and the analysis for langasite resonators has not been conducted.

In this article, the frequency shift of a langasite resonator with arbitrary orientation under DC electric field is discussed based on concepts regarding small fields superposed on finite-biasing fields in a thermoelectroelastic body [15] and perturbation theory [16]. The complete set of third-order material constants—including third-order elastic, piezoelectric, dielectric, and electrostrictive constants—is needed for this calculation. The contributions of nonlinear material constants to the electroelastic effect of langasite resonators are analyzed for several crystal cuts. By comparing the contribution of each group of nonlinear material constants to the electroelastic effect, specific cuts of interest are identified with respect to the nonlinear material constants.

In the next section, the first-order perturbation integral theory is introduced. The general solution of the dynamic response of an infinite, thin piezoelectric plate without DC biasing electric field is obtained in the third section. The static stress, strain, and electric field distribution of a doubly-rotated langasite plate under a biasing static electric field in the thickness direction are obtained analytically and numerically in the fourth section. In the fifth section, the electroelastic effect and sensitivity analysis are obtained both analytically and by the finite-element method. Conclusions are made in the sixth section.

II. Perturbation Integral

The resonant frequency of a resonator depends on its geometry, material constants, and boundary conditions. When a langasite resonator is subjected to an external biasing electric field, the geometry changes slightly because of the electromechanical effect. In this case, the material constants may be characterized as effective constants, which will change with the biasing electric field. Thus, the biasing electric field will cause a shift of resonant frequency, a value that may be estimated accurately by perturbation integral theory. The expression to estimate a specific mode can be found from [16]:

Manuscript received September 21, 2006; accepted May 4, 2007. This research was supported by the Army Research Office under Grant No. DAAD19-01-1-0443.

H. Zhang, J. A. Turner, and J. Yang are with the Department of Engineering Mechanics, University of Nebraska-Lincoln, Lincoln, NE 68588-0526 (e-mail: hfzhang@bigred.unl.edu).

J. A. Kosinski is with the U.S. Army Research Development and Engineering Command (RDECOM) Communications-Electronics Research, Development and Engineering Center (CERDEC), Fort Monmouth, NJ 07703-5211.

Digital Object Identifier 10.1109/TUFFC.2007.507

$$\begin{aligned}\Delta\omega_M &= \omega - \omega_M \\ &= \frac{1}{2\omega_M \int \rho_0 \left(u_1^M u_1^M + u_2^M u_2^M + u_3^M u_3^M\right) dV} \\ &\quad \times \int_V \left(\hat{c}_{K\alpha L\gamma} u^M_{\gamma,K} u^M_{\alpha,L} + 2\hat{e}_{KL\gamma}\varphi^M_K u^M_{\gamma,L}\right. \\ &\quad \left. - \hat{\varepsilon}_{KL}\varphi^M_{,K}\varphi^M_{,L}\right) dV,\end{aligned} \tag{1}$$

where:

$$\begin{aligned}\hat{c}_{K\alpha L\gamma} &= T^0_{KL}\delta_{\alpha\gamma} + c_{K\alpha LN} w_{\gamma,N} + c_{KNL\gamma} w_{\alpha,N} \\ &\quad + c_{K\alpha L\gamma AB} S^0_{AB} + k_{AK\alpha L\gamma} E^0_A,\end{aligned} \tag{2}$$

$$\hat{e}_{KL\gamma} = e_{KLM} w^0_{\gamma,M} - k_{KL\gamma AB} S^0_{AB} + b'_{AKL\gamma} E^0_A, \tag{3}$$

$$\hat{\varepsilon}_{KL} = b'_{KLAB} S^0_{AB} + \chi_{KLA} E^0_A, \tag{4}$$

with:

$$b'_{AKL\gamma} = b_{ABCD} + \varepsilon_0 \delta_{AB}\delta_{CD} - \varepsilon_0(\delta_{AC}\delta_{BD} + \delta_{AD}\delta_{BC}).$$

In (1)–(4), ω_M is the unperturbed angular frequency, ω is the perturbed angular frequency, and $\Delta\omega_M$ is the angular frequency shift. Here, $\hat{c}_{K\alpha L\gamma}$, $\hat{e}_{KL\gamma}$, and $\hat{\varepsilon}_{KL}$ are the effective elastic, piezoelectric, and dielectric constants, respectively; u^M_γ is a specific mode shape function under the unperturbed condition and φ^M is the electric potential for this specific mode. T^0_{KL}, S^0_{AB}, E^0_A are the initial stress, strain, and electric field, respectively, with $w_{\gamma,N}$ defining the displacement gradient. $c_{K\alpha L\gamma}$, d_{fAB}, ε_{KL} are the second-order elastic, piezoelectric and dielectric constants. $c_{K\alpha L\gamma AB}$, $k_{fK\alpha L\gamma}$, and χ_{KLf} are the third-order elastic, piezoelectric, and dielectric constants respectively, and $b_{fAL\gamma}$ are the electrostrictive constants. ε_0 is the permittivity of free space. It is worth noting that the definition of the energy density used here differs from that of Sorokin *et al.* [17]. The resulting differences in material constants are discussed in the Appendix.

The displacement gradient is the summation of strain and the rigid body rotation tensor. It may be written:

$$w_{\gamma,N} = S_{\gamma N} + \Omega_{\gamma N}.$$

Physically, it can be easily verified that a rotation of the position of a crystal resonator will not cause a resonant frequency shift. Theoretically, it was proven in [18] that an arbitrary pure homogeneous infinitesimal rigid body rotation has no influence on frequency shift. Thus, in the case considered here, the displacement gradient may be obtained directly from the static strain solution.

The frequency shift, as given by (1), is a function of the mode, the natural frequency without perturbation, and the effective material constants. From (2)–(4), the effective materials constants are functions of electric field E, as well as the initial stress and strain. Thus, estimates of the frequency shift of a resonator under a DC electric field require the mode shape and electric distribution potential for the resonator. Then, the static solution for the electric field, initial stress, and strain are required. These solutions may be obtained analytically or numerically.

For a resonator with simple geometry, the perturbation integral (1) may be simplified greatly. But for a resonator with relatively complex geometry, the perturbation integral can be carried out only numerically. In such cases, the finite-element solution combined with numerical integration may be done to estimate the resonator frequency shift accurately. The initial stress, strain, and electric field can be solved by the finite-element method for element stress, strain, and electric field. The volume integral can be treated as the summation of each element volume. The perturbation integral for the finite-element approach may be expressed as:

$$\Delta\omega_M = \Delta\omega_1 + \Delta\omega_2 - \Delta\omega_3, \tag{5}$$

where:

$$\begin{aligned}\Delta\omega_1 &= \sum_{N=1}^{ELN} (T^0_{KL}(N)\delta_{\alpha\gamma} + 2c_{K\alpha LN} S^0_{\gamma N}(N) \\ &\quad + c_{K\alpha L\gamma AB} S^0_{AB}(N) + k_{AK\alpha L\gamma} E^0_A(N) \\ &\quad + 2c_{K\alpha LN}\Omega^0_{\gamma N}(N)) u^M_{\gamma,K}(N) u^M_{\alpha,L}(N) V(N), \\ \Delta\omega_2 &= 2\sum_{N=1}^{ELN} (e_{KLM}(S^0_{\gamma M}(N) + \Omega^0_{\gamma M}(N)) \\ &\quad - k_{KL\gamma AB} S^0_{AB}(N) \\ &\quad + b'_{AKL\gamma} E^0_A(N))\varphi^M_K(N) u^M_{\gamma,L}(N) V(N), \\ \Delta\omega_3 &= \sum_{N=1}^{ELN} (b'_{KLAB} S^0_{AB}(N) \\ &\quad + \chi_{KLA} E^0_A(N))\varphi^M_{,K}(N)\varphi^M_{,L}(N) V(N).\end{aligned}$$

Here, N is the element number and $T^0_{KL}(N)$, $S^0_{\gamma N}(N)$, $E^0_A(N)$, $V(N)$ are the element stress, strain, electric field and volume. The rigid body rotation tensor $\Omega^0_{\gamma N}(N)$ is calculated from the nodal displacements. The analytical solution to be derived in Section III is used for the mode shape $u_k(N)$ and electric field $\varphi(N)$.

III. Unperturbed Response

Consider the free vibrations of a thin plate cut from a single crystal with arbitrary symmetry, as shown schematically in Fig. 1. The plate is fully coated with electrodes on both sides. The boundary conditions are assumed traction free. The governing equations may be written:

$$c_{2jk2} u_{k,22} + e_{22j}\varphi_{,22} = \rho\ddot{u}_j, \tag{6}$$

$$e_{2k2} u_{k,22} - \varepsilon_{22}\varphi_{,22} = 0. \tag{7}$$

The boundary conditions are written:

$$T_{2j} = c_{2jk2} u_{k,2} + e_{22j}\varphi_{,2} = 0, \tag{8}$$

$$\varphi = 0, \text{ at } x_2 = \pm h. \tag{9}$$

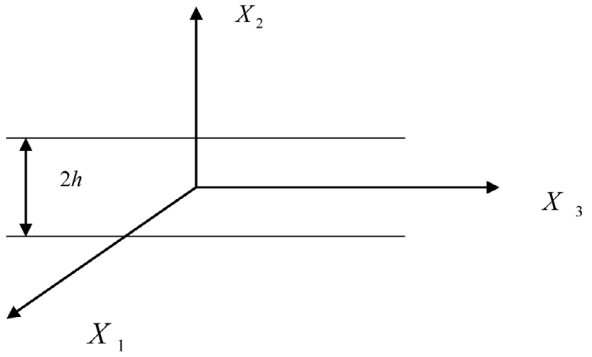

Fig. 1. A doubly-rotated langasite plate with electrodes on both sides.

The general solution for this case can be summarized as:

$$u_j(x_2,t) = \sum_{i=1}^{3} D_j^i \sin\lambda_i x_2 e^{-i\omega t} = \sum_{i=1}^{3} K^i B_j^i \sin\lambda_i x_2 e^{-i\omega t}, \quad j = 1,2,3, \tag{10}$$

$$\varphi(x_2,t) = \sum_{i=1}^{3} \left(K^i \frac{e_{11m}}{\varepsilon_{11}} B_m^i \sin\lambda_i x_2 + P_1 x_2 + P_2 \right) e^{-i\omega t}, \quad m = 1,2,3. \tag{11}$$

where:

$$P_1 = -\frac{1}{h} \sum_{i=1}^{3} K^i \frac{e_{11m}}{\varepsilon_{11}} B_m^i \sin\lambda_i h, \tag{12}$$

$$P_2 = 0. \tag{13}$$

Thus, the ith mode shape may be defined as:

$$u_j^i(x_2) = D_j^i \sin\lambda_i x_2. \tag{14}$$

The amplitudes D_j^i are obtained by solving the eigenvalue problem:

$$(c'_{2jk2} - c\delta_{jk}) D_k = 0,$$

where:

$$c'_{2jk2} = c_{2jk2} + (e_{22j} e_{22k})/\varepsilon_{22}.$$

Here, $(u_j^i(x_2))^M = B_j^i \sin\lambda_i x_2$ is the ith normalized mode shape and K^i is the normalized weighting coefficient, $\lambda_i = \sqrt{\rho\omega^2/c_1}$, with ω as the angular frequency. Substituting (10) and (11) into boundary conditions (8) and (9) gives the transcendental equation which is used to determine the resonant frequency. This equation is:

$$Det\{ B_m^i [c'_{2jk2} \omega h \sqrt{c^i/\rho} \cos(\omega h \sqrt{c^i/\rho}) - (e_{22j} e_{22m}/\varepsilon_{22}) \sin\omega h \sqrt{c^i/\rho}] \} = 0. \tag{15}$$

Eq. (15) is solved numerically for the frequencies of interest to find the natural frequency. Alternatively, the resonant frequency can be approached by the antiresonant frequency as [19]:

$$\omega \approx \omega_1 = \frac{(2q-1)}{4h} \sqrt{\frac{c_j}{\rho}}, \quad j = 1,2,3, \quad q = 1,2,3\ldots. \tag{16}$$

Eq. (16) is often an accurate approximation for any overtone for materials with low piezoelectric coupling coefficient. For materials with high piezoelectric coupling coefficient, the approximation is ideal for high overtones ($q \geq 4$). Langasite has moderately high piezoelectric coupling. Therefore, (16) is expected to apply for high overtones.

IV. Biasing Electric Field

When a DC electric field is applied in the thickness direction, the biasing electric field gives rise to static strain, stress, and electric field solutions. For resonators with simple geometry, such as the plano-plano configuration considered here, the solution may be obtained by analytical methods. However, for resonators with relatively complex geometry, such as plano-convex or double bevel configurations, the solution may be obtained by finite-element methods. It is worth noting that the analytical solutions ignore edge effects that can be obtained by the finite-element method.

A. Analytical Solution

Consider a doubly-rotated langasite plate fully coated with electrodes on both sides as shown in Fig. 1. A static voltage $\pm V/2$ is applied on the upper and lower surfaces of the plate. The material orientation is shown in Fig. 2, which follows the IEEE standard [19]. The linear constitutive equations of piezoelectricity can be written [20]:

$$S_{ij}^0 = s_{ijkl} T_{kl}^0 - d_{kij} E_k^0, \tag{17}$$

$$D_i^0 = d_{ikl} T_{kl}^0 + \varepsilon_{ik} E_k^0, \tag{18}$$

$$T_{ji,j}^0 = 0, \tag{19}$$

$$D_{i,i}^0 = 0, \tag{20}$$

where the strain and the electric field are written:

$$S_{kl}^0 = (w_{k,l} + w_{l,k})/2, \tag{21}$$

$$E_k^0 = -\varphi_{,k}^0. \tag{22}$$

In (21) and (22), w_k is the displacement component and φ^0 is the electric potential. The boundary conditions are written:

$$\varphi^0 = \pm V/2, \quad x_2 = \pm h, \tag{23}$$

$$T_{2j}^0 = 0, \quad x_2 = \pm h. \tag{24}$$

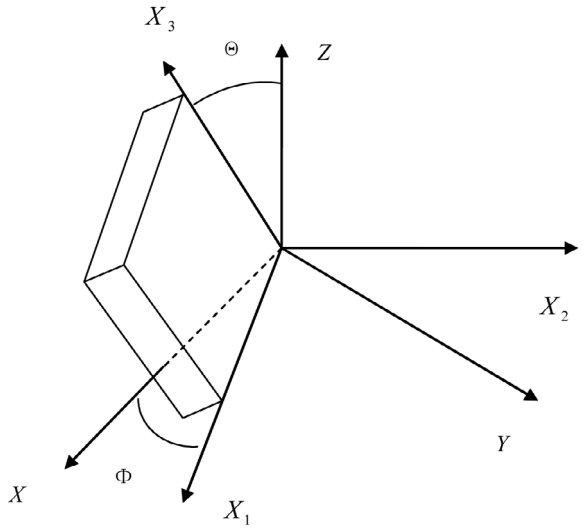

Fig. 2. Plate orientation of a doubly-rotated langasite resonator (YXwl Φ/Θ).

Consider a possible solution for an infinite, thin plate as: $T^0_{ij} = 0$, $S^0_{ij} = K_{ij} = \text{constant}$, $\varphi^0_{,k} = F_k = \text{constant}$ in Ω. Obviously, the boundary conditions as given by (23) and (24) are satisfied, as are the equations of motion, (19) and (20). The static solutions are obtained as:

$$S^0_{ij} = d_{kij} E^0_k \text{ in } \Omega, \tag{25}$$

$$T^0_{ij} = 0 \text{ in } \Omega, \tag{26}$$

$$E^0_k = -\frac{V}{2h} \text{ in } \Omega. \tag{27}$$

B. Finite-Element Solution

A finite-element model for a doubly-rotated (YXwl $\Omega = 20°/\Theta = 30°$) langasite resonator is constructed using FEMLAB 3.2 (COMSOL, Inc., Burlington, MA). The model includes 2224 Lagrangian quadratic elements with the number of boundary elements as 1640, such that there are three layers of elements. The sample radius is 6.5 mm, the thickness is 0.65 mm, and a 1000 V DC voltage is applied along the plate thickness direction. A voltage of this magnitude is appropriate for the example results calculated here. Such a voltage is simple to implement experimentally and results in a natural frequency shift (in the range of 0.07–1.5 Hz/V) that can be measured easily. The radial edge of the plate has zero charge. The convergence of the numerical solution is verified by refining the element size and by comparison with the analytical solutions. In the analytical solution, the strain, stress, and field are assumed to be uniform based on the thin plate theory. An example finite-element result, shown in Fig. 4 shows the shear strain S_{12}. The solution is basically uniform (solid gray throughout most of the plate) except for some edge effects (darker gray near the edges).

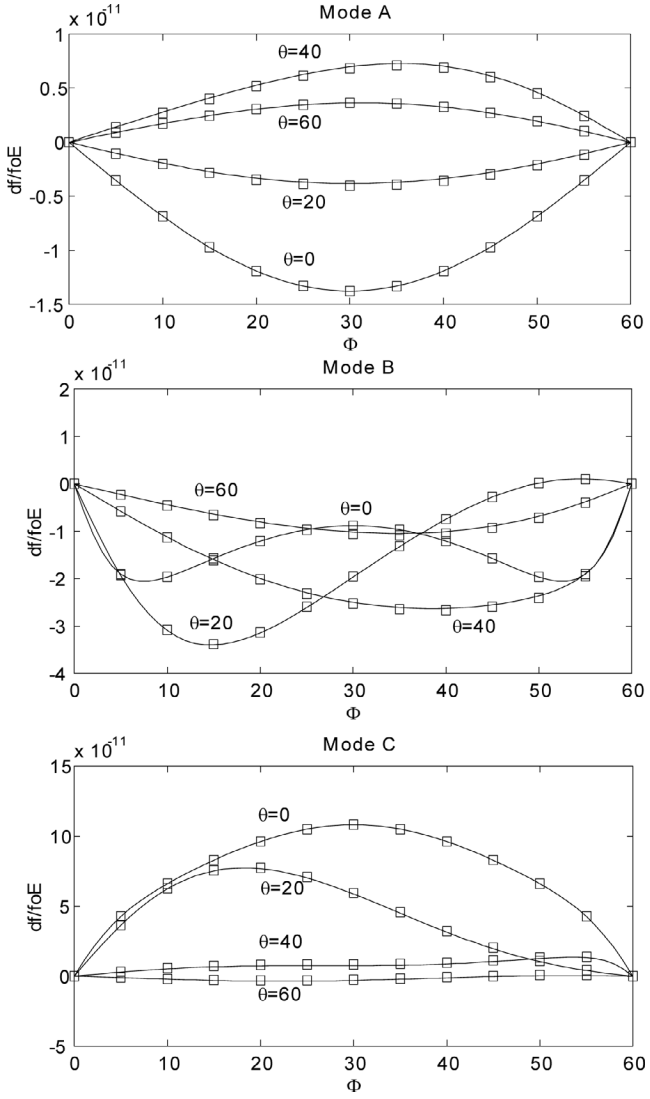

Fig. 3. Electroelastic effect of LGS thickness mode resonator (YXwl Φ/Θ).

V. Results

After the unperturbed natural frequency, mode shape, static stress, strain, and field are obtained. All material constants are transformed to the new coordinate. Then (1) and (5), respectively, may be used for the calculation of the electroelastic effect analytically and numerically. Example results are presented in this section.

A. Electroelastic Effect

The results for the electroelastic effect are shown in Fig. 3. The electroelastic effect is represented by df/f_0E, where, df is the natural frequency shift, f_0 is the natural frequency without any biasing electric field, and E is the electric field. For each mode [mode A (longitudinal), mode B (fast shear), mode C (slow shear)], the electroelastic effect is plotted for four groups of resonator orientations: YXwl $\Phi = 0° - 60°/\Theta = 0°$, YXwl $\Phi = 0° - 60°/\Theta = 20°$, YXwl $\Phi = 0° - 60°/\Theta = 40°$, YXwl $\Phi = 0° - 60°/\Theta = 60°$,

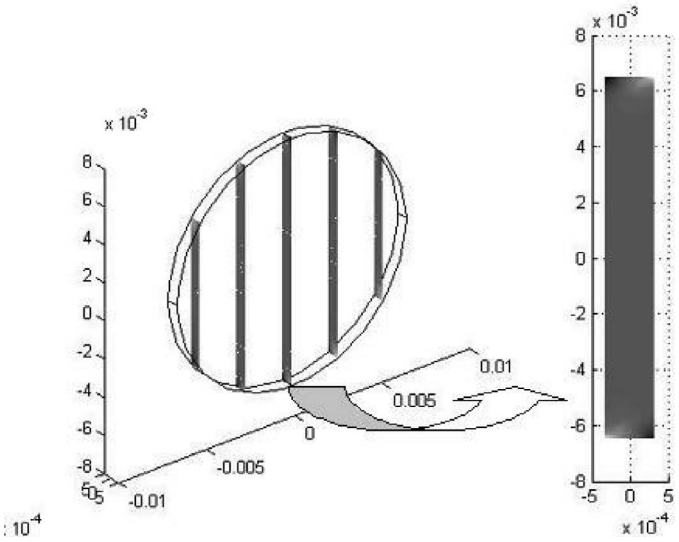

Fig. 4. Static solution for shear strain S_{12} determined by the finite-element method.

respectively. The solid line is the analytical result. The squares denote the finite-element results. As expected, the electroelastic effect changes smoothly with cut angle. The comparison between the finite-element result and the analytical result shows the consistency of these two methods. A slight difference between these two methods is observed that can be explained by the zero stress assumption for the analytical stress solution. Edge effects also contribute to this difference. The intersection of the curve with the X axis shows a possible cut that is insensitive to the electric field. This crossing point is not observed for Modes A or Modes C. Such a cut exists only for cut YXwl $\Phi = 50°/\Theta = 20°$ in Mode B. It is worth noting that the electroelastic effect of Mode C is much larger in magnitude than the other two modes. Thus, mode C of cut YXwl $\Phi = 30°/\Theta = 0°$ may be an ideal mode for voltage sensor applications.

B. Sensitivity to Nonlinear Material Constants

Results showing the electroelastic effect for select langasite resonators using both analytical and numerical solutions are now presented. Because the interest here is on the behavior with respect to third-order material constants, only the contribution to the electroelastic effect from third-order material constants is presented such that contributions from second-order material constants are excluded. Figs. 5–8 show the analytical and numerical results of the electroelastic effect for modes A, B, and C. Cut angles of $\theta = 0°$, $20°$, $40°$, $60°$ are shown in Figs. 5–8 respectively, for $\Phi = 0° - 60°$. The analytical results are shown as solid lines. The numerical results are denoted with a square. The first observation of the results is that the numerical results fit all analytical results very well. Thus, it may be concluded that the assumptions used in the analysis are sufficient for the resonators considered here. Specific observations of the results for each cut also may be made.

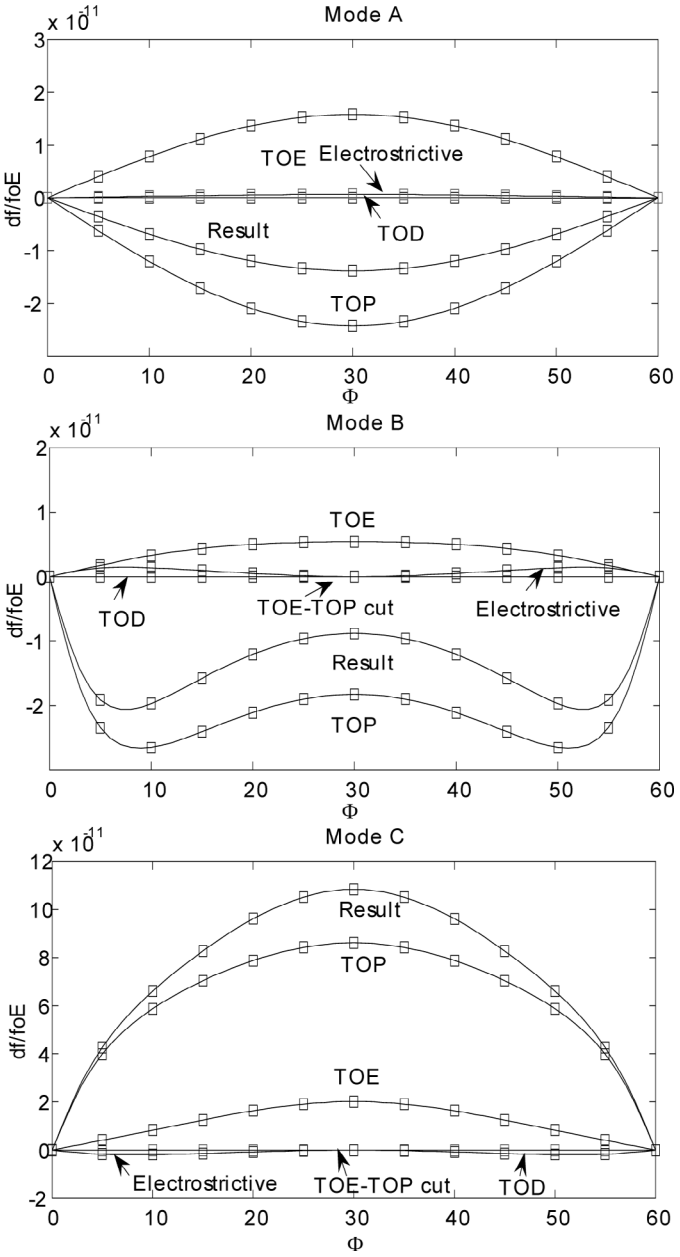

Fig. 5. Contribution to electroelastic effect from nonlinear material constants for YXwl $\Phi = 0° - 60°/\Theta = 0$. The notation used includes TOE (third-order elastic constants), TOP (third-order piezoelectric constants), TOD (third-order dielectric constants), Electrostrictive (electrostrictive constants).

Fig. 5 shows the electroelastic effect for the YXwl $\Phi = 0° - 60°/\Theta = 0°$. The results for Mode A (longitudinal mode) show that the primary contributions to the frequency shift come from third-order elastic and piezoelectric effects with little contribution from electrostrictive constants and no effective contribution from the third-order dielectric constants. For Mode B, it may be observed that the cuts YXwl $\Phi = 25° - 35°/\Theta = 0°$ have zero contribution from the electrostrictive constants, such that this cut range could be termed the "third-order elastic-piezoelectric cut (TOE-TOP cut)." Thus, these cuts are ideal for experimental measurements to determine third-

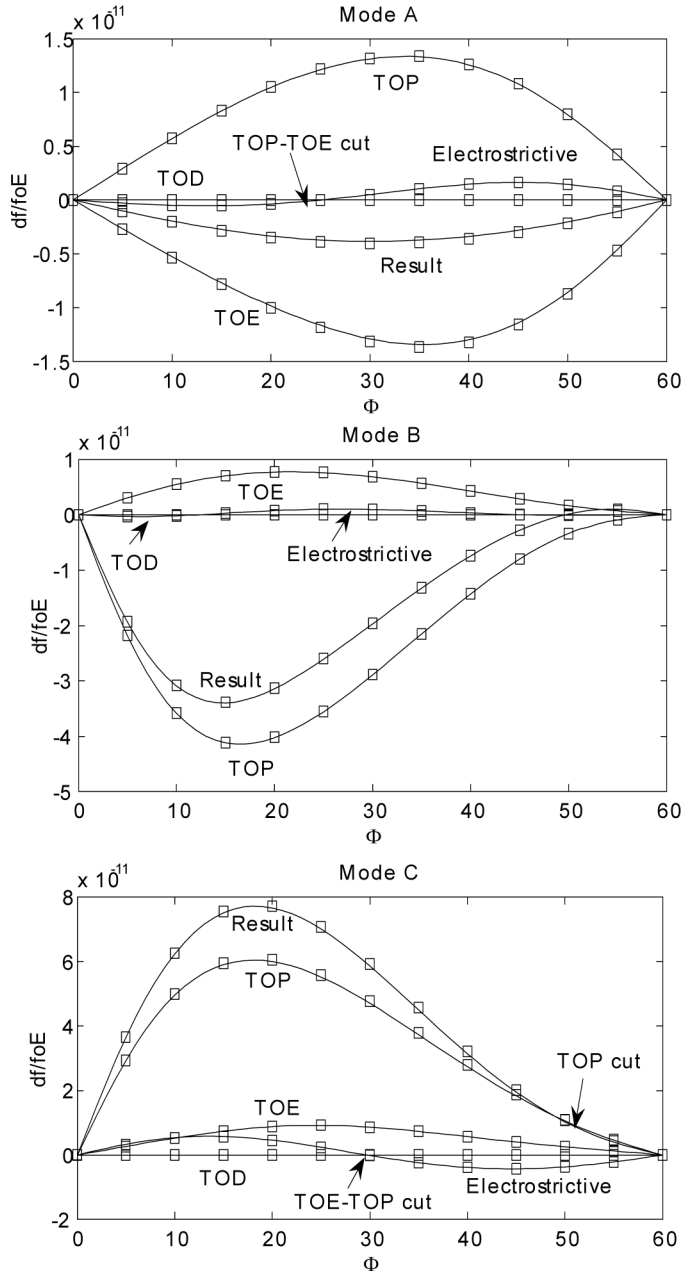

Fig. 6. Contribution to electroelastic effect from nonlinear material constants for YXwl $\Phi = 0° - 60°/\Theta = 20°$. The notation used includes TOE (third-order elastic constants), TOP (third-order piezoelectric constants), TOD (third-order dielectric constants), Electrostrictive (electrostrictive constants).

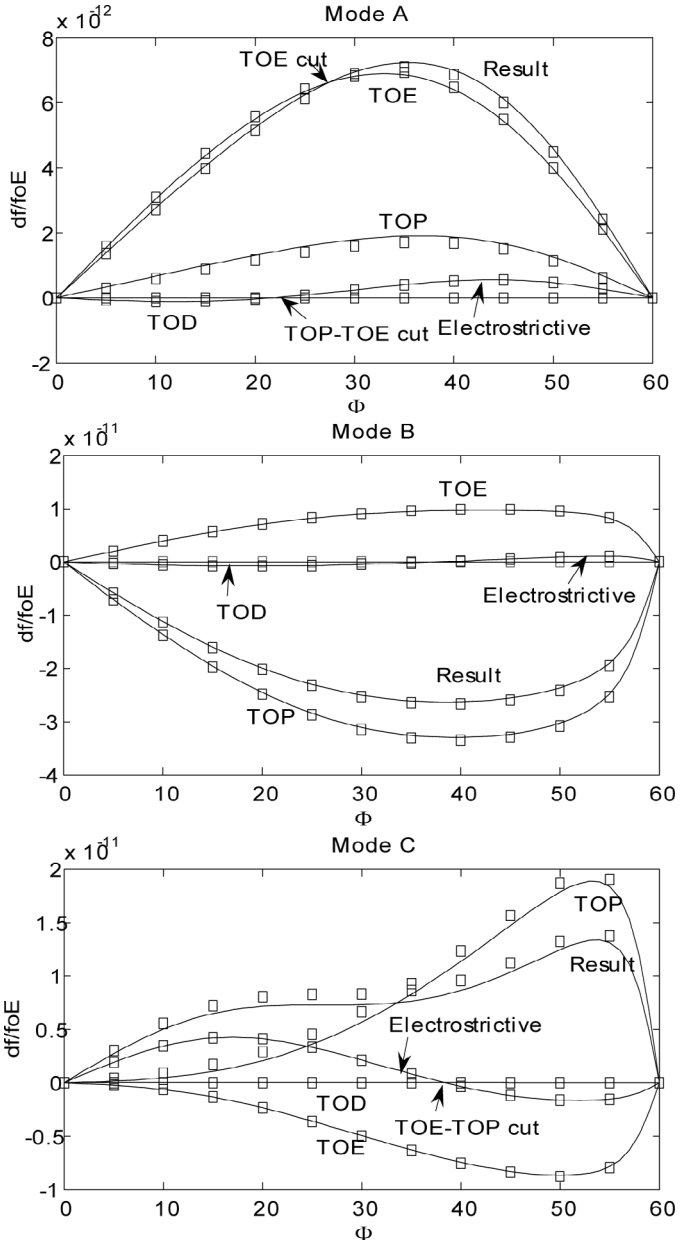

Fig. 7. Contribution to electroelastic effect from nonlinear material constants for YXwl $\Phi = 0° - 60°/\Theta = 40°$. The notation used includes TOE (third-order elastic constants), TOP (third-order piezoelectric constants), TOD (third-order dielectric constants), Electrostrictive (electrostrictive constants).

order elastic and piezoelectric constants without the need to consider the influence of electrostrictive constants. For Mode C, the same cut range also exists. Fig. 6 shows the results for cuts YXwl $\Phi = 0° - 60°/\Theta = 20°$. Compared with the YXwl $\Phi = 0° - 60°/\Theta = 0°$ cuts, these cuts have a larger contribution from electrostrictive constants. For Mode A, cut YXwl $\Phi = 25°/\Theta = 20°$ may be designated as a "third-order elastic-piezoelectric cut (TOE-TOP cut)." It also should be noted that, for Mode C, cut YXwl $\Phi = 48°/\Theta = 20°$ (the crossing point) is a "third-order piezoelectric constants cut (TOP cut)," because the electroelastic response is the same as that obtained by considering effects from third-order piezoelectric constants only. Special cuts for other values of Θ also are expected and require further investigation. In Fig. 7, we notice in Mode C, the influence of the electrostrictive constants to electroelastic effect is the largest for the cut range YXwl $\Phi = 0° - 22°/\Theta = 40°$. It even surpasses the contribution from the third-order elastic and piezoelectric constants. Therefore, this cut range may be appropriate for determination of electrostrictive constants if third-order elastic and piezoelectric constants are known. In Fig. 8, YXwl $\Phi = 25°/\Theta = 60°$ of Mode C is the "third-order elastic

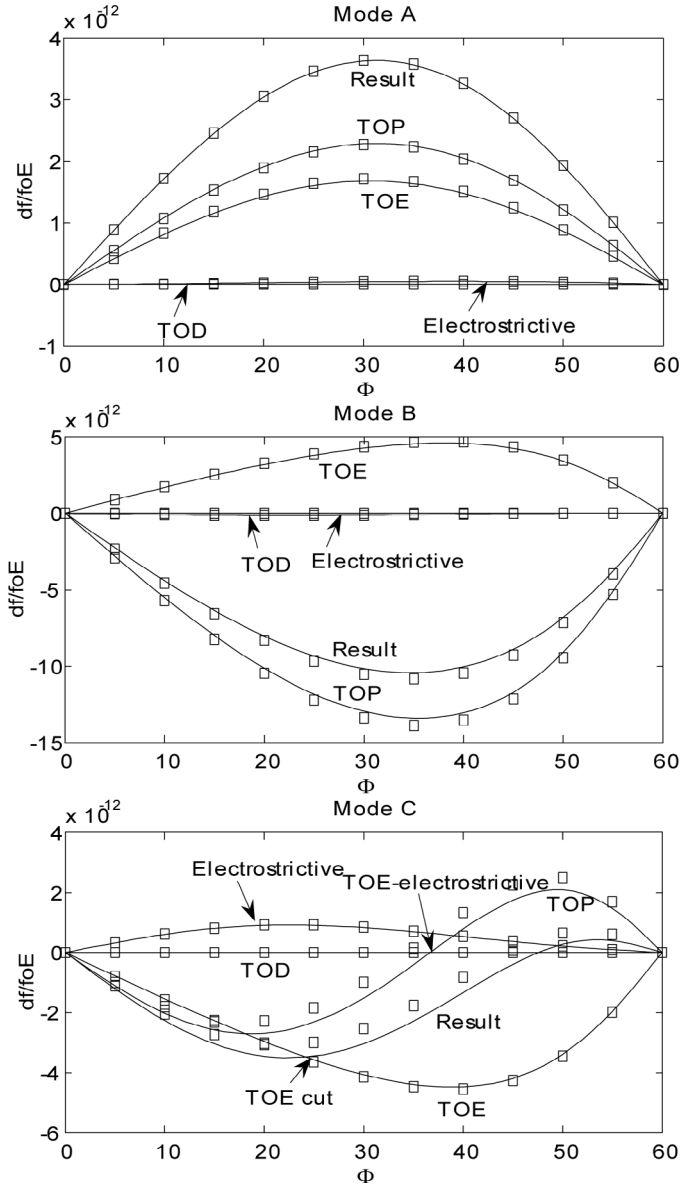

Fig. 8. Contribution to electroelastic effect from nonlinear material constants for YXwl $\Phi = 0° - 60°/\Theta = 60°$. The notation used includes TOE (third-order elastic constants), TOP (third-order piezoelectric constants), TOD (third-order dielectric constants), Electrostrictive (electrostrictive constants).

constants cut (TOE cut)". We note that, for cut YXwl $\Phi = 35°/\Theta = 60°$, the third-order piezoelectric constants have zero contribution to the electroelastic effect, which means that this cut can be used to determine electrostrictive and third-order elastic constants. This cut may be denoted as a "electrostrictive-third-order elastic constants cut".

VI. Conclusions

Analytical and finite-element solution for determining the electroelastic effect and the sensitivity analysis of thickness mode langasite resonator are obtained. The FEM results were shown to fit the analytical results very well for the range of cuts examined. Thus, the applicability of the assumptions necessary for the analytical solution was verified for plano-plano resonator configurations. The results show the cut that may be used for the case when the frequency stability is required when the resonator is exposed to external field. There also exist possible cuts for voltage sensor applications. The contribution to the electroelastic effect from each group of constants depends on the cut angle and mode. Overall, it was observed that the third-order dielectric constants contribute little to the electroelastic effect. The major contribution usually comes from third-order elastic and piezoelectric constants. Also, there exist special cuts that are dominated by a specific group of constants such as a "third-order elastic constants cut" or a "third-order piezoelectric constants cut." A pure "electrostrictive constants cut" was not observed for the cases examined. The contribution from electrostrictive constants is generally small, although some cuts did have a significant contribution that cannot be ignored. The results from this analysis provide valuable insight into the sensitivity of the electroelastic effect to the nonlinear material behavior.

Appendix A

A. Energy Density Definition

The energy density is defined here as [21]:

$$\begin{aligned}\rho_0\psi(S_{KL}, E_K) &= \frac{1}{2}c_{ABCD}S_{AB}S_{CD} \\ &\quad - e_{ABC}E_A S_{BC} - \frac{1}{2}\chi_{AB}E_A E_B, \\ &+ \frac{1}{6}c_{ABCDEF}S_{AB}S_{CD}S_{EF} + \frac{1}{2}k_{ABCDE}E_A S_{BC}S_{DE} \\ &\quad - \frac{1}{2}b_{ABCD}E_A E_B S_{CD} - \frac{1}{6}\chi_{ABC}E_A E_B E_C, \quad (28)\end{aligned}$$

where the material constants c_{ABCD}, e_{ABC}, χ_{AB}, c_{ABCDEF}, k_{ABCDE}, b_{ABCD}, and χ_{ABC} are called the second-order elastic, piezoelectric, electric susceptibility, third-order elastic, third-order piezoelectric, electrostrictive and third-order dielectric, respectively. This energy definition does not include the energy density in a vacuum. However, the energy definition given in [17] is the total electric enthalpy that includes the energy density in a vacuum. Thus, the definition of material constants differs from [17]. These constants must be modified before they can be used in the calculations presented. Table I lists the modifications needed. The complete set of materials constants of Langasite with respect to crystallographic axes X, Y, and Z are available in [17], and are listed in Tables II–VIII.

References

[1] Q. Chen, T. Zhang, and Q.-M. Wang, "Frequency-temperature compensation of piezoelectric resonators by electric dc bias

TABLE I
A COMPARISON BETWEEN DIFFERENT MATERIAL CONSTANT DEFINITIONS.

Material constants	[17]	Here
2nd elastic	c_{ABCD}	c_{ABCD}
2nd piezoelectric	e_{ABC}	e_{ABC}
2nd dielectric	$\chi_{AB}+\varepsilon_0\delta_{AB}$	χ_{AB}
3rd elastic	c_{ABCDEF}	c_{ABCDEF}
3rd piezoelectric	$-k_{ABCDE}$	k_{ABCDE}
3rd dielectric	χ_{ABC}	χ_{ABC}
electrostrictive	$b_{ABCD}+\varepsilon_0\delta_{AB}\delta_{CD}$ $-\varepsilon_0(\delta_{AC}\delta_{BD}+\delta_{AD}\delta_{BC})$	b_{ABCD}

TABLE II
SECOND-ORDER ELASTIC CONSTANTS OF LANGASITE (10^{10} N/M^2).

c_{11}	18.875	c_{24}	1.412
c_{12}	10.475	c_{33}	2.614
c_{13}	9.589	c_{44}	5.35
c_{14}	−1.412	c_{55}	5.35
c_{22}	18.875	c_{56}	−1.412
c_{23}	9.589	c_{66}	4.2

TABLE III
SECOND-ORDER PIEZOELECTRIC CONSTANTS OF LANGASITE (C/M^2).

e_{11}	−0.44	e_{21}	0	e_{31}	0
e_{12}	0.44	e_{22}	0	e_{32}	0
e_{13}	0	e_{23}	0	e_{33}	0
e_{14}	−0.08	e_{24}	0	e_{34}	0
e_{15}	0	e_{25}	0.08	e_{35}	0
e_{16}	0	e_{26}	0.44	e_{36}	0

TABLE IV
SECOND-ORDER DIELECTRIC CONSTANTS (10^{-12} C/VM).

ϵ_{11}	167.52
ϵ_{22}	167.52
ϵ_{33}	448.92

TABLE V
FOURTEEN INDEPENDENT THIRD-ORDER ELASTIC CONSTANTS OF LANGASITE (10^{10} N/M^2).

c_{111}	−97.2	c_{134}	−4.1
c_{112}	0.7	c_{144}	−4.0
c_{113}	−11.6	c_{155}	−19.8
c_{114}	−2.2	c_{222}	−96.5
c_{123}	0.9	c_{333}	−183.4
c_{124}	−2.8	c_{344}	−38.9
c_{133}	−72.1	c_{444}	20.2

TABLE VI
EIGHT INDEPENDENT THIRD-ORDER PIEZOELECTRIC CONSTANTS OF LANGASITE (C/M^2).

e_{111}	9.3	c_{124}	−4.8
e_{113}	−3.5	e_{134}	6.9
e_{114}	1.0	e_{144}	−1.7
e_{122}	0.7	e_{315}	−4

TABLE VII
THIRD-ORDER DIELECTRIC PERMEABILITY (10^{-20} F/V).

χ_{111}	−0.5

TABLE VIII
THIRD-ORDER ELECTROSTRICTIVE CONSTANTS OF LANGASITE (10^{-11} N/V^2).

H_{11}	−26	H_{31}	−24
H_{12}	65	H_{33}	−40
H_{13}	20	H_{41}	−170
H_{14}	−43	H_{44}	−44

field," *IEEE Trans. Ultrason., Ferroelect., Freq. Contr.*, vol. 52, pp. 1627–1631, Oct. 2005.
[2] M. Ishido, K. Ojima, and N. Kikuta, "Electrostatic voltage sensor and displacement sensor, using SAW directional coupler," in *Proc. IEEE Ultrason. Symp.*, 1991, pp. 341–344.
[3] M. Ishido and X. Zhu, "Electrostatic voltage sensor using SAW osillator with waveguide," in *Proc. IEEE Ultrason. Symp.*, 1987, pp. 383–387.
[4] R. Bauerschmidt and P. Lerch, "Optical voltage sensor based on a quartz resonator," in *Proc. IEEE Ultrason. Symp.*, 1996, pp. 383–387.
[5] Y. K. Yong and M. S. Patel, "Application of a dc-bias to reduce acceleration sensitivity in quartz resonators," *Int. J. Appl. Electromagn. Mechan.*, vol. 22, pp. 69–82, 2005.
[6] C. K. Hruska, "The electroelastic constants of quartz determined by the resonator method," *J. Appl. Phys.*, vol. 65, pp. 715–717, Jan. 1989.
[7] N. Naumenko, "Optimal cuts of langasite, $La_3Ga_5SiO_{14}$ for SAW devices," *IEEE Trans. Ultrason., Ferroelect., Freq. Contr.*, vol. 48, no. 2, pp. 530–537, Mar. 2001.
[8] M. Adachi, T. Kimura, W. Miyamoto, Z. Chen, and A. Kawabata, "Dielectric, elastic and piezoelectric properties of $La_3Ga_5SiO_{14}$ (LANGASITE) single crystals," *J. Korean Phys. Soc.*, vol. 32, pp. S1274–S1277, 1998.
[9] R. C. Smythe, "Langasite, langanite, and langatate bulk-wave y-cut resonators," *IEEE Trans. Ultrason., Ferroelect., Freq. Contr.*, vol. 47, no. 2, pp. 355–360, Mar. 2000.
[10] H. Fritze, M. Schulz, H. Seh, and H. Tuller, "High temperature operation and stability of langasite resonators," in *Proc. Mater. Res. Soc. Symp.*, 2005, pp. 157–162.
[11] I. Mateescu, J. Zelenka, J. Nosek, and G. Johnson, "Frequency-temperature characteristics of the langasite resonators," in *Proc. Annu. IEEE Int. Freq. Contr. Symp.*, 2001, pp. 263–267.
[12] Y. Kim and A. Ballato, "Force-frequency effect of y-cut langanite and y-cut langatate," *IEEE Trans. Ultrason., Ferroelect., Freq. Contr.*, vol. 50, pp. 1678–1682, Dec. 2003.
[13] J. A. Kosinski, R. A. Pastore, Jr., X. Yang, J. Yang, and J. A. Turner, "Stress-induced frequency shifts in langasite thickness-mode resonators," in *Proc. Annu. IEEE Int. Freq. Contr. Symp.*, 2003, pp. 716–722.
[14] R. Brendel, "Material nonlinear piezoelectric coefficients for quartz," *J. Appl. Phys.*, vol. 54, pp. 5339–5346, 1983.
[15] J. Yang, "Equations for small fields superposed on finite biasing fields in a thermoelectroelastic body," *IEEE Trans. Ultrason., Ferroelect., Freq. Contr.*, vol. 50, no. 2, pp. 187–192, 2003.
[16] H. Tiersten, "Perturbation theory for linear electroelastic equations for small fields superposed on a bias," *J. Acoust. Soc. Amer.*, vol. 64, pp. 832–837, 1978.
[17] B. P. Sorokin, P. P. Turchin, S. I. Burkov, D. A. Glushkov, and K. S. Alexandrov, "Influence of static electric field, mechanical pressure and temperature on the propagation of acoustic waves in $La_3Ga_5SiO_{14}$ piezoelectric single crystal," in *Proc. IEEE Int. Freq. Contr. Symp.*, 1996, pp. 161–169.
[18] H. F. Tiersten and B. K. Sinha, "Temperature dependence of the resonant frequency of electrode doubly rotated quartz thickness-

mode resonators," *J. Acoust. Soc. Amer.*, vol. 50, pp. 8038–8051, 1979.
[19] *IEEE Standard on Piezoelectricity, ANSI/IEEE Std. 176-1987*, 1987.
[20] H. F. Tiersten, *Linear Piezoelectric Plate Vibration*. New York: Plenum, 1969.
[21] J. Yang, *An Introduction to the Theory of Piezoelectricity. Advances in Mechanics and Mathematics*. Band 9. New York: Springer-Verlag, 2005.

Haifeng Zhang received his B.S. in Engineering Mechanics from Hunan University, Changsha, China in 1997 and his M.S. in Solid Mechanics from Northwestern Polytechnical University, Xian, China in 2001, he obtained his Ph.D. degree in Engineering Mechanics from University of Nebraska, Lincoln, NB, in 2007.

Joseph A. Turner was born in Iowa Falls, Iowa in 1965. He received the B.S. degree in engineering science and the M.Engr. degree in engineering mechanics, both in 1988 from Iowa State University, Ames, Iowa. He received the Ph.D. degree in theoretical and applied mechanics (T&AM) in 1994 from the University of Illinois at Urbana-Champaign (UIUC), Urbana, IL.

He is currently an Associate Professor in the Department of Engineering Mechanics at the University of Nebraska-Lincoln, Lincoln, NE, where he began as an Assistant Professor in 1997. Prior to that he was an Alexander von Humboldt Postdoctoral Research Fellow from 1995–1996 at the Fraunhofer Institute for Nondestructive Testing in Saarbrücken, Germany and a postdoctoral research associate in T&AM at UIUC from 1994–1995.

He is an associate member of the American Society of Mechanical Engineers and an associate member of the Acoustical Society of America.

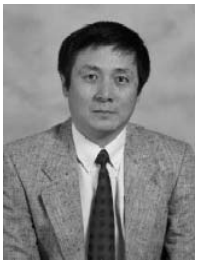

Jiashi Yang received his B.E. and M.E. in engineering mechanics in 1982 and 1985 from Tsinghua University, Beijing, China, and his Ph.D. in civil engineering in 1994 from Princeton University, Princeton, NJ. He was a Postdoctoral Fellow from 1993 through 1994 at the University of Missouri-Rolla, Rolla, MO, and from 1994 through 1995 at Rensselaer Polytechnic Institute, Troy, NY. He was employed by Motorola, Inc., Schaumburg, IL, during 1995 through 1997.

Since 1997 he has been an Assistant and Associate Professor at the Department of Engineering Mechanics of the University of Nebraska-Lincoln, Lincoln, NE. Dr. Yang has published over 170 journal papers on electromechanical materials and devices, and three books: *An Introduction to the Theory of Piezoelectricity*, *The Mechanics of Piezoelectric Structures*, and *Analysis of Piezoelectric Devices*. He is an Associate Editor of the *IEEE Transactions on Ultrasoncis, Ferroelectrics, and Frequency Control*.

John A. Kosinski (A'86–M'88–SM'91–F'03) received the A.A. degree in science in 1978 from Ocean County College, Toms River, NJ, the B.S. degree in physics in 1980 from Montclair State College, Upper Montclair, NJ, the M.S. degree in electronic engineering in 1988 from Monmouth College, West Long Branch, NJ, and the Ph.D. degree in electrical engineering in 1993 from Rutgers, the State University of New Jersey, Piscataway, NJ.

Since 1981 he has served as a civilian employee of the U.S. Army at Fort Monmouth, NJ, first at the U.S. Army Electronics Technology and Devices Laboratory, and subsequently at the U.S. Army Communications-Electronics Research, Development, and Engineering Center (CERDEC). His research career has touched upon many areas of interest to the IEEE UFFC Society, including the development and characterization of new piezoelectric materials, design of bulk (BAW), Rayleigh wave (SAW), and surface transverse wave (STW) devices for simultaneously high-Q, low acceleration sensitivity, and temperature compensation, improved voltage-controlled oscillator circuit designs, and tunable/programmable SAW filters and modules. He has collaborated on studies of loss in piezoelectric ceramics, application of ultrasonics to electromagnetic interference (EMI) suppression, and novel micro-electromechanical (MEM) mounting structures.

Dr. Kosinski has received the Department of the Army Research and Development Achievement Award six times for work in the areas of SAW device acceleration sensitivity; electrodiffusion processing of quartz material; high-power microwave EMI protection; understanding of the fundamental nature of acceleration sensitivity in phase coherent signal sources; the development of electronics for tactical unmanned aerial vehicles; and the application of information theory to a military identification problem. He received the Superior Civilian Service Award for his role in a specially equipped team deployed to the World Trade Center to assist in victim rescue and evidence recovery in response to the terrorist attacks of September 11, 2001.

Dr. Kosinski is a Fellow of the IEEE and has been both an elected member of the UFFC Society Administrative Committee (ADCOM) and an Associate Editor of these *Transactions*. He currently serves on the technical program committee of the IEEE International Ultrasonics Symposium and will be General Chair for the 2007 Symposium. He has published more than 150 technical articles, including numerous invited papers and tutorials, and holds 19 United States patents. Dr. Kosinski is a Senior Research Fellow and Director of Admissions for the International Society for Philosophical Enquiry (ISPE), a global non-profit organization dedicated to the advancement of human knowledge through personal accomplishment, advanced enquiry, and creative contributions.